View metadata, citation and similar papers at core.ac.uk
brought to you by CORE
provided by E-resource repository of the University of Latvia

Ion track template technique for fabrication of $ZnSe_2O_5$ nanocrystals

A. Akilbekov[1], A.Akylbekova[1], A. Usseinov[1], A. Kozlovskyi[1,2], Z. Baymukhanov[1], Sh. Giniyatova[1], A.I. Popov[3], A. Dauletbekova[1]

[1]L.N. Gumilyov Eurasian National University, Nur-Sultan, Kazakhstan

[2]Institute of Nuclear Physics, Nur-Sultan, Kazakhstan

[3]Institute of Solid State Physics University of Latvia, Riga, Latvia

Abstract. $ZnSe_2O_5$ nanocrystals with an orthorhombic structure were synthesized by electrochemical deposition into a-SiO_2/n-Si ion track template formed by 200 MeV Xe ion irradiation with the fluence of 10^7 ions/cm^2. The lattice parameters determined by the X-ray diffraction and calculated by the CRYSTAL computer program package are very close to each other. It was shown that $ZnSe_2O_5$ has a direct band gap of 2.8 eV at the Γ-point. In addition, the calculated charge distribution and chemical bonds show that the crystal has an ion-covalent nature. The photoluminescence excited by photons at 300 nm has a low intensity arising mainly due to zinc and oxygen vacancies.

Introduction

Ion track technologies are currently a powerful approach for producing new macro- and nanomaterials. From the very beginning, they were based on the idea of using ion tracks [1-4]. Ion tracks and related color centers were observed and studied in detail in a large number of different materials [5-14]. The most striking and impressive application of this technology is

associated with the creation of polymer track membranes, the so-called nuclear membranes [15-17]. The current demand and requirements for nuclear membranes are already high and will grow rapidly. Nuclear membranes are obtained by irradiation with heavy ions of a polymer film followed by their physicochemical treatment. As a result, the initial film turns into a microfiltration membrane with through pores of a cylindrical shape. These systems are widely used in physics, medicine and biology [18]. In particular, nuclear membranes with pores measuring 0.5–1 μm in size are widely used for analytical purposes in physicochemical studies as well as in biological and medical experiments, while membranes with pores of diameter 0.1–0.2 μm are used to make filters for fine purification of technological materials in semiconductor device electronics. On the other hand, structures with the smallest pores (<0.1 μm) are used in the technique of thorough gas processing and in the microbiological industry [15 -18]. Note that the controlled formation of pores in technological materials is very important problem for various areas of modern electronics [19-21].

In recent years, using the method of template synthesis, nuclear membranes have been successfully used for the fabrication of various nanomaterials, including, in particular, Ni, Pt, Cu, Ag and Au nanotubes [22] as well as also Ag, Cu, Pt [23], Ni, Ag, Au, Zn and Cu nanoparticles [24 - 28]. In addition to polymeric materials, a-SiO_2/Si structures have also been frequently and successfully used as ion track templates. Then, using a-SiO_2/Si as a templates, the following structures, such as Au metal nanoclusters [29], Ni and Cu nanoparticles [30], zinc oxide nanocrystals [31, 32], or CdTe nanocrystals [9, 33] were successfully obtained.

Thus, this method is still promising and successful for the engineering and design of semiconductor materials based on compounds A^3B^5 and A^2B^6 for their integration into silicon technology and possible use for micro-, opto- and nanoelectronics [2,3, 16-18].

In this work, using the method of electrochemical deposition on the track template a-SiO_2/Si, the formation of zinc diselenide nanocrystals is reported. It can be expected that the synthesized $ZnSe_2O_5$ nanocrystal will not only have properties similar to ZnO and ZnSe, but will also

exhibit their own specific and unique characteristics. Therefore, it can be expected that the data obtained will arouse interest in studying the possibility of using $ZnSe_2O_5$ nanocrystals as various active elements in sensors, optoelectronic and nanoelectronic systems that can be currently developed.

Experimental

The a-SiO2 / n-Si substrates, in which a is amorphous and n is the type of conductivity, were obtained by thermal oxidation of the (Si-n) disk in a humid oxygen atmosphere at 900 ° C with the formation of an oxide layer thickness of 700 nm. Then, samples made with a size of 1x1 cm were irradiated with 200 MeV Xe ions to a fluence of 10^7 ions/cm^2 at a DC-60 cyclotron (Nur-Sultan, Kazakhstan).

Chemical etching of irradiated a-SiO2 / n-Si samples was carried out in a 4% aqueous solution of HF with the addition of palladium *(*m(Pd)=0.025 g) at 18°± 1°C. Before and after etching of ion tracks, ultrasonic cleaning (6.SB25-12DTS) of the sample surface in isopropanol was carried out for 15 minutes. After processing, the samples were washed in deionized water (18.2 MΩ). The analysis of nanopores after etching was carried out using a scanning electron microscope (SEM) JSM-7500F.

Electrochemical deposition (ECD) $ZnSe_2O_5$ was carried out, using the following electrolyte: $ZnSO_4 \times 7\ H_2O$ – 7.2 g/l; SeO_2 – 0.2 g/l. Firstly, $ZnSO_4$ and SeO_2 were dissolved in deionized water, then two solutions were mixed. For the electrochemical synthesis of nanostructures, a two-electrode cell with zinc cathodes was used, the distance between which is fixed. The process of nanostructure formation in the templates was controlled using the method of chronoamperometry, which consists in controlling the increase in the electric current a a function of time as the pores of the template are filled. Thus the growth of nanostructures was monitored by chronoamperometry using an Agilent 34410A multimeter. The deposition voltage was found to be U = 1.25 V, the voltage that is used to fill the nanopores. X-ray

diffraction analysis (XRD) of the samples was carried out on a D8 ADVANCE ECO X-ray diffractometer. The photoluminescence (PL) spectra were recorded, using an Agilent Technologies spectrofluorimeter (Cary Eclipse Fluorescence Spectrophotometer) in spectral range from 300 nm to 800 nm at room temperature at 300 nm excitation.

Results and discussion

First of all, ECD was performed on 6 samples that had previously been subjected to ion irradiation. As an example, Figure 1 shows the SEM images of two samples after ECD. Corresponding analysis of SEM images showed that the number of filled nanopores is on average 80%.

[Figure 1]

Subsequent X-ray diffraction study of all 6 samples revealed the formation of single-phase $ZnSe_2O_5$ nanocrystals characterized by an orthorhombic crystal structure and belonging to the Pbcn (60) space group, as shown in Table 1.

[Table 1]

The lattice parameters obtained above for the orthorhombic unit cell of $ZnSe_2O_5$ are in good agreement with the corresponding data for single crystals [34]. In [35], the preparation of polycrystalline ZnSe films by the chemical deposition (CD) method was made depending on the pH level of the solution, which varied from 8 to 11. In particular, at pH = 11 the simultaneous formation of three phases was found : ZnSe, $ZnSe_2O_5$ and $ZnSeO_3$, while only the two phases ZnSe and $ZnSe_2O_5$ are remained with a pH decrease. It should be noted that there are no detailed reports on $ZnSe_2O_5$, which is clearly related to the difficulty of its preparation in a single-phase state.

To verify the above experimental data for $ZnSe_2O_5$, we also performed *non-empirical* calculations of the $ZnSe_2O_5$ crystal in the approximation of linear combinations of atomic orbitals (LCAO) using the exchange-correlation functional within local density approximation (LDA) [36, 37]. The calculations were performed in the CRYSTAL program [38]. This

computer program performs calculations of the electronic structure of crystalline systems using the Hartree-Fock methods, density functional (DFT) and various hybrid approximations in combination with the basis set of local (Gaussian) functions for periodic (3D, 2D, 1D) systems and has established itself as a reliable tool to describe the different properties of a wide range of materials.

To describe the atoms of $ZnSe_2O_5$ crystal, the following Gaussian-type basic sets were chosen: the Jaffe basis [39] for the zinc (Zn) and oxygen (O) atoms, and the Towler basis [40] for the selenium (Se) atom. In order to better describe both the structural and electronic properties, the upper *sp*-orbital from original Se basis was removed.

It is known that for a correct description of the electronic structure of a crystal, it is necessary to accurately determine the total energy of the crystal cell [41, 42]. In CRYSTAL calculations high convergence tolerances for the Coulomb and exchange integrals have been chosen for the Coulomb overlap (10^{-7}), Coulomb penetration (10^{-7}), exchange overlap (10^{-7}), first exchange pseudo overlap (10^{-7}), and the second exchange pseudo overlap (10^{-14}).

The effective atomic charges and bond population were calculated using the Mulliken analysis [43].

[Figure 2.]

We have used a periodic supercell model of a primitive $ZnSe_2O_5$ cell, consisting of 32 atoms (Fig. 2). The calculated lattice parameters (*a*, *b*, *c*), crystal density (ρ_V), and effective atomic charges (q_{eff}) are presented in Table 2 together with experimental results.

[Figure 3]

Figure 3 shows the band structure of the crystal together with the density of the electronic states (DOS). As follows from the Fig.3, the bandgap energy of $ZnSe_2O_5$ is 2.8 eV (which is

close to earlier calculated value of 3.04 eV [44]) and that the band gap is direct at the Γ point of the Brillouin zone. In addition, as clearly seen from DOS, the valence band is represented mainly by O 2p orbitals, while the conduction band mainly consists of Zn 3d, 4s and Se 3d, 4s orbitals, which indicates at essentially ionic compound. However, charge distribution analysis shows also significant covalent contribution to the Se-O chemical bonding in the crystal.

Finally, we performed test measurements of the luminescent properties of $ZnSe_2O_5$, which can be expected as a symbiosis of the luminescence of both zinc oxide and zinc selenide. From the luminescent point of view, a qualitative analysis of the structure of $ZnSe_2O_5$ (Fig. 2) shows that in its luminescence, the contribution due to ZnO should be more predominant than the contribution from the luminescence of ZnSe, since, as follows from the crystal structure of $ZnSe_2O_5$, the Zn-Se bond is realized through O.

Figure 4 shows the differential PL spectrum after ECD, which displays all the common features for all 6 deposited samples. A comparison of this spectrum with the PL spectra of ZnO [45-48] and ZnSe [49] allows us to assume that the PL band with a maximum of 500 nm (2.48 eV) (green luminescence) can be due to oxygen vacancies (V_O) as in ZnO [43], while the band with a maximum of 422 nm (2.94 eV) (blue luminescence), is due to zinc vacancies (V_{Zn}) [43] in ZnO. Thus, the PL band with a maximum of 422 nm can be associated with zinc vacancies (V_{Zn}) in the $ZnSe_2O_5$ lattice. In the X-ray and photoluminescence spectra of ZnSe single crystals, wide recombination bands with peaks at 626 and 963 nm have been observed [44]. In our case, the PL band has also a maximum at 635 nm (1.95 eV). In the case ZnSe, similar feature has been assigned to a complex center consisting of a zinc vacancy and an impurity small donor V_{Zn} + D [49].

For a detailed interpretation of the photoluminescence spectra, it is necessary to carry out detailed measurements and analysis of the corresponding luminescence excitation spectra, which will be the subject of further research.

Conclusions

The $ZnSe_2O_5$ nanocrystals obtained by the method of electrochemical deposition into a 200 MeV Xe ion track template (a-SiO_2/n-Si) have an orthorhombic crystal structure and crystal lattice parameters coinciding with those for the single crystals. In addition, using the CRYSTAL computer program package, the $ZnSe_2O_5$ lattice parameters were also calculated, which were found to be almost close to experimental ones. It was also shown that $ZnSe_2O_5$ reveals the direct-band gap of 2.8 eV at the Γ –point. In addition, the calculated charge distribution and chemical bonds show that the crystal has an ion-covalent nature. The PL excited by light at 300 nm showed a low intensity and is mainly due to zinc and oxygen vacancies.

Acknowledgment. The work was performed under the grant of the Ministry of Education and Science of the Republic of Kazakhstan AP05134367 and Latvian grant lzp xxx .

References

1. D. Fink, L.T. Chadderton, K. Hoppe, W.R. Fahrner, A. Chandra, A. Kiv, Nucl. Instr. and Meth. B, 261 (2007) 727.
2. D. Fink, A. Petrov, H. Hoppe, W.R. Fahrner, R.M. Papaleo, A.Berdinsky, A. Chandra, A. Biswas, L.T. Chadderton, Nucl. Instr. and Meth. B, 218 (2004) 355.
3. D. Fink, A. Petrov, W.R. Fahrner, K. Hoppe, R.M. Papaleo, A. Berdinsky, A. Chandra, A. Zrineh, L.T. Chadderton, Int. J. Nanosci, 4 (2005) 965.
4. K. Hoppe, W.R. Fahrner, D. Fink, S. Dhamodoran, A. Petrov, A. Chandra, A. Saad, F. Faupel, V.S.K. Chakravadhanula, V. Zaporotchenko, Nucl. Instr. and Meth. B, 266 (2008) 1642.
5. A. Dauletbekova, K. Schwartz, M.V. Sorokin, A. Russakova, M. Baizhumanov, A. Akilbekov, M. Zdorovets, M. Koloberdin, Nucl. Instr. Meth. B, 326 (2014) 311.
6. A. Dauletbekova, K. Schwartz, M.V. Sorokin, J. Maniks, A. Rusakova, M. Koloberdin, A. Akilbekov, M. Zdorovets, Nucl. Instr. Meth. B, 295 (2013) 89.
7. M.L. Crespillo, F. Agulló-López, A. Zucchiatti, Nucl. Instr. Meth. B, 394 (2017) 20.
8. K. Kimura, S. Sharma, A.I. Popov, Nucl. Instrum. Meth. B, 191 (2002) 48; Radiat. Meas., 34 (2001) 99.
9. R. Balakhaeva, A. Akylbekov, A. Dauletbekova, A. Kozlovsky, Z. Baymukhanov, Sh. Giniyatova and A. Useinov, AIP Conference Proceedings, 2174 (2019) 020006.
10. A.J. van Vuuren, M.M. Saifulin, V.A. Skuratov, J.H. O'Connell, G. Aralbayeva, A. Dauletbekova, M. Zdorovets, Nucl. Instr. Meth. B, 460 (2019) 67.
11. G. Szenes, F. Paszti, A. Peter, A.I. Popov, Nucl. Instr. Meth. B, 166–167 (2000) 949
12. A. Popov, E. Balanzat, Nucl. Instr. Meth. B, 166 (2000) 545.
13. D.V. Ananchenkoa, S.V. Nikiforov, V.N. Kuzovkov, A.I. Popov, G.R. Ramazanova, R.I. Batalov, R.M. Bayazitov, H.A. Novikov, Nuclear Inst. Meth. B, 466 (2020) 1-7,
14. R.S. Averback, P. Ehrhart, A.I. Popov, A. Von Sambeek, Radiation Effects and Defects in Solids, 136 (1995) 169.

15. P.Y. Apel. Track-Etching. Encyclopedia of Membrane Science and Technology, Wiley, (2013) p.25.
16. P. Apel, Radiation measurements, 34 (2001) 559-566.
17. G.N. Flerov, P.Y. Apel, A. Y., Didyk, V.I. Kuznetsov, R.T. Oganesyan. Soviet Atomic Energy, *67* (1989) 763-770.
18. M.V. Hoek (Ed.) and V.V. Tarabara (Ed.) Track-Etching. Encyclopedia of Membrane Science and Technology, Part IV. Membrane Applications, Wiley, (2013) p.2390.
19. J.A. Suchikova, Journal of Nano-and Electronic Physics, 7(2015), 03017.
20. Y.A Suchikova, V.V. Kidalov, G.A. Sukach, Journal of Nano- and Electronic Physics, 1(4) (2009) 78-86
21. Y.O. Suchikova, Journal of Nano- and Electronic Physics, 9(2017) 01006
22. L.Velleman, J.G. Shapter, D. Losic, J. Membr. Sci., 328 (2009) 121.
23. F. Muench, M. Oezaslan, T. Seidl, S. Lauterbach, P. Strasser, H.-J. Kleebe, W. Ensinger, Appl. Phys. A, 105 (2011) 847.
24. I. Enculescu, M. Sima, M. Enculescu, E. Matei, M.E. Toimil Molares, Th. Cornelius. Optoelectron. Adv. Mat., 2 (2008) 133.
25. P. Shao, J. Membr. Sci., 255 (2005) 1.
26. V. Kumar, R.Singh, S.K. Chakarvarti, Dig. J. Nanomater. Biostruct., 2 (2007) 163.
27. M. Pashchanka, R.C. Hoffmann, A. Gurlo, J.C. Swarbrick, J. Khanderi, J. Engstler, A. Issanin, J.J. Schneider, Dalton Trans., 40 (2011) 4307.
28. D.B. Kadyrzhanov, M.V. Zdorovets, A.L. Kozlovskiy, L.E. Kenzhina, A.V. Petrov, Mater. Res. Express., 4 (2017) 125023.
29. P. Kluth, B. Johannessena, C.J. Glover, M.C. Foran, Ridgway. Nucl. Instr. Meth. B., 238 (2005) 285.
30. Yu.A. Ivanova, D.K. Ivanou, A.K. Fedotov, E.A. Streltsov, S.E. Demyanov, A.V. Petrov, E.Yu. Kaniukov , J Mater Sci., 42 (2007) 9163.

31. A. Dauletbekova, L. Vlasukova, Z. Baimukhanov, A. Akilbekov, A. Kozlovskiy, Sh. Giniyatova, A. Seitbayev, A. Usseinov, A. Akylbekova, Phys. stat. sol. B, 256 (2019) 1800408.
32. Sh. Giniyatova, A. Dauletbekova, Z. Baimukhanov, L. Vlasukova, A. Akilbekov, A. Usseinov, A. Kozlovskiy, A. Akylbekova, Radiation measurements, 125 (2019) 52.
33. D.K. Ivanou, E.A. Streltsov, A.K. Fedotov, A.V. Mazanik, D. Fink, A. Petrov, Thin Solid Films, 490 (2005) 154.
34. G. Meunier, M. Bertaud, Acta Crystallographica. Section B, 30 (1974) 2840.
35. F.M. Tezel, İ.A. Kariper, International Journal of Modern Physics B, 33 (2019) 1950024
36. P.A.M. Dirac, Proc. Cambridge Phil. Soc. (1930) 376.
37. J. P. Perdew, A. Zunger, Phys. Rev. B, (1981) 5048.
38. R. Dovesi, V.R. Saunders, R. Roetti, R. Orlando, C.M. Zicovich-Wilson, F. Pascale, B. Civalleri, K. Doll, N.M. Harrison, I.J. Bush, P. D'Arco, M. Llunell. CRYSTAL14 User's Manual University of Torino, Torino (2014).
39. J.E. Jaffe, A.C. Hess, Phys.Rev. B, 48 (1993) 7903.
40. Selenium basis set for Crystal Program, (http://www.tcm.phy.cam.ac.uk/~mdt26/basis_sets/Se_basis.txt)
41. F. Gallino, G. Pacchioni, and C. Di Valentin, J. Chem. Phys., 133 (2010) 144512.
42. C.G. Van de Walle and J. Neugebauer, Appl. Phys. Lett., 95 (2008) 3851.
43. R.S. Mulliken. J. Chem, Phys., 23 (1955) 1833.
44. A. Jain, S.P. Ong, G. Hautier, W. Chen, W.D. Richards, S. Dacek, S. Sholia, D. Gunter, D. Skinner, G. Ceder and K.A. Persson, APL Materials, 1 (2013) 011002.
45. A.V. Uklein, V.V. Multian, G.M. Kuz'micheva, R.P. Linnik, V.V. Lisnyak, A.I. Popov, V.Ya. Gayvoronsky, Opt. Mater., 84 (2018) 738.
46. B. El Filali, J.A. Jaramillo Gomez, T.V. Torchynska, J.L. Casas Espinola, L. Shcherbyna, Opt. Mater, 89 (2019) 322.

47. S.A. Studenikin, N. Golego, M. Cocivera, J. Appl.Phys., 84 (1998) 2287

48. H. Kumano, A.A. Ashrafi, A. Ueta, A. Avramescu, I. Suemune, J. Cryst. Growth, 214/215 (2000) 280.

49. V.Ya. Degoda, A.O. Sofienko, Semiconductors, 44 (2010) 1.

Figure captions

Figure 1. SEM images of the surface and the transverse cleavage of two samples deposited at 1.25 V (a, c — surfaces, b, d — cross section).

Figure 2. Atomic structure of $ZnSe_2O_5$ unit cell (32 atoms). The boundaries of the cell and the directions of the translation vectors are shown.

Figure 3. Density of states and band structure of pure $ZnSe_2O_5$ crystal. The horizontal dashed lines indicate the limits of the valence and conduction bands.

Figure 4. Differential PL spectra after ECD of $ZnSe_2O_5$.

Table 1. Parameters of $ZnSe_2O_5$ nanocrystals

№	Phase	Structure type	Space group	(hkl)	2θº	d, Å	Cell parameters, Å	Degree of crystallinity %
1	$ZnSe_2O_5$	Orthorhombic	Pbcn(60)	113	47.669	1.90623	a=6.84898, b=10.40588 c=6.10726	60
				161	56.573	1.62550		
2	$ZnSe_2O_5$	Orthorhombic	Pbcn(60)	222	43.532	2.07729	a=6.82438, b=10.30182 c=6.08451	62
				161	56.668	1.62301		
3	$ZnSe_2O_5$	Orthorhombic	Pbcn(60)	161	56.605	1.62467	a=6.83702, b=10.34424 c=6.10479	65,1
4	$ZnSe_2O_5$	Orthorhombic	Pbcn(60)	161	56.668	1.62301	a=6.82495, b=10.30976 c=6.16404	62
5	$ZnSe_2O_5$	Orthorhombic	Pbcn(60)	222	43.596	2.07442	a=6.77276, b=10.41286 c=6.18404	76
				115	47.985	1.89442		
				161	56.637	1.62384		
6	$ZnSe_2O_5$	Orthorhombic	Pbcn(60)	222	43.564	2.07585	a=6.71034, b=10.34140 c=6.24588	58,6
				161	56.637	1.62384		

Table 2. Calculated parameters of $ZnSe_2O_5$ crystal

Parameter	This work, (calculations)	This work, (experiment)	[29] (experiment)
a, Å	6.86	6,71034 Å	6.797 ± 0.002 Å
a, Å	6.86	6,71034 Å	6.797 ± 0.002 Å
b, Å	10.14	10,34140 Å	10.412 ± 0.003 Å
c, Å	5.77	6,24588 Å	6.068 ± 0.002 Å
Space group	*Pbcn*	*Pbcn*	*Pbcn*
ρ_V (g/cm^3)	4.971	-	4.44
q_{eff} (Zn/Se/O)	+1.23/+1.41/-0.833	-	-

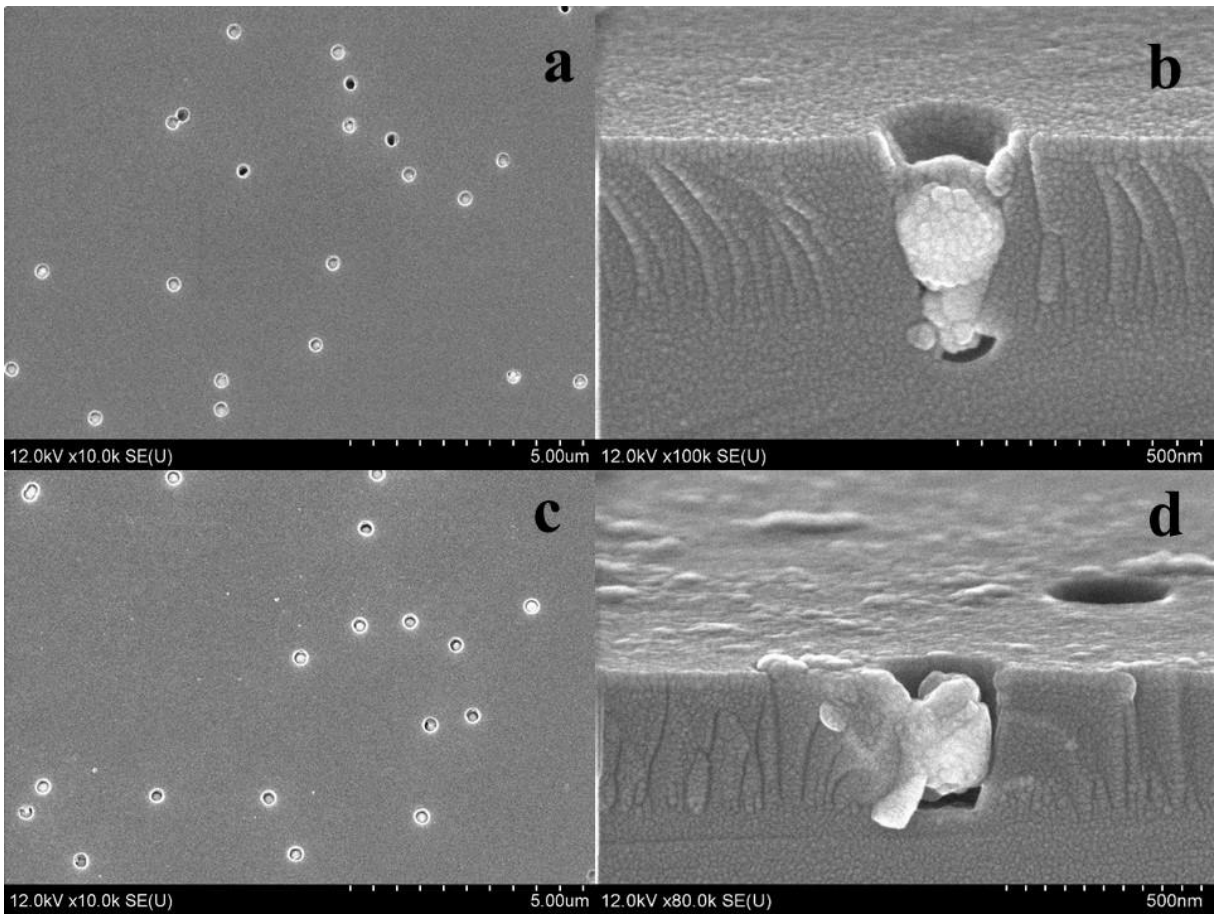
a
b
12.0kV x10.0k SE(U)
5.00um
12.0kV x100k SE(U)
500nm
c
d
12.0kV x10.0k SE(U)
5.00um
12.0kV x80.0k SE(U)
500nm

Fig.1.

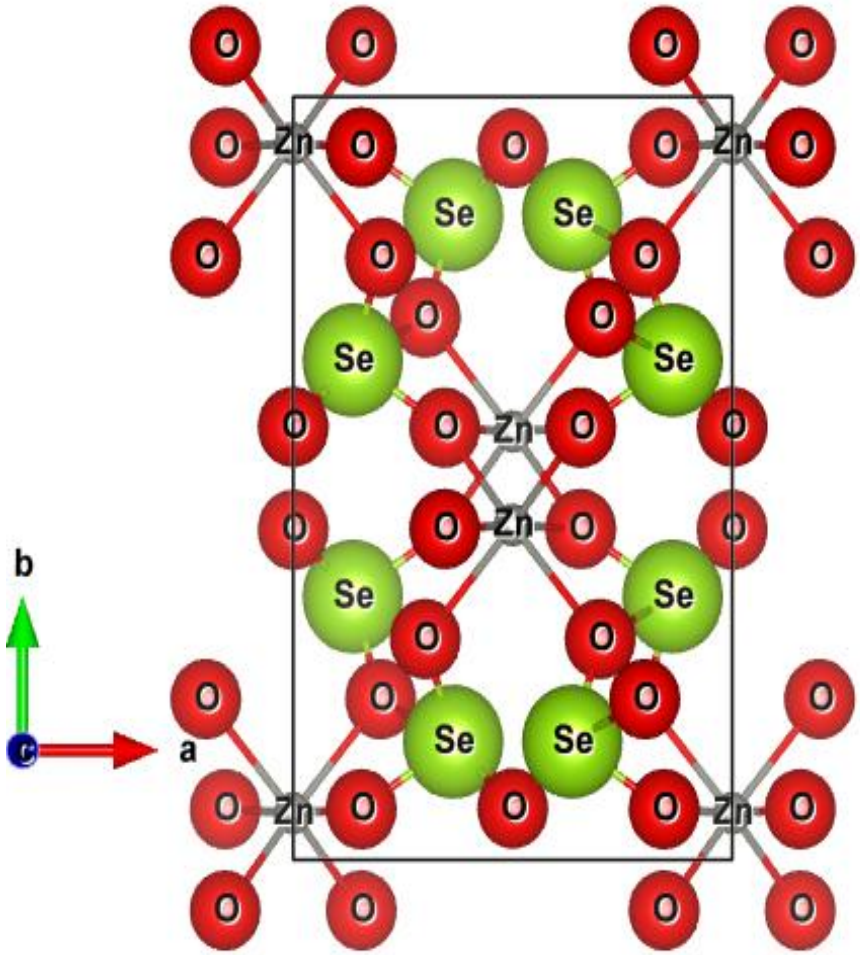

Fig. 2.

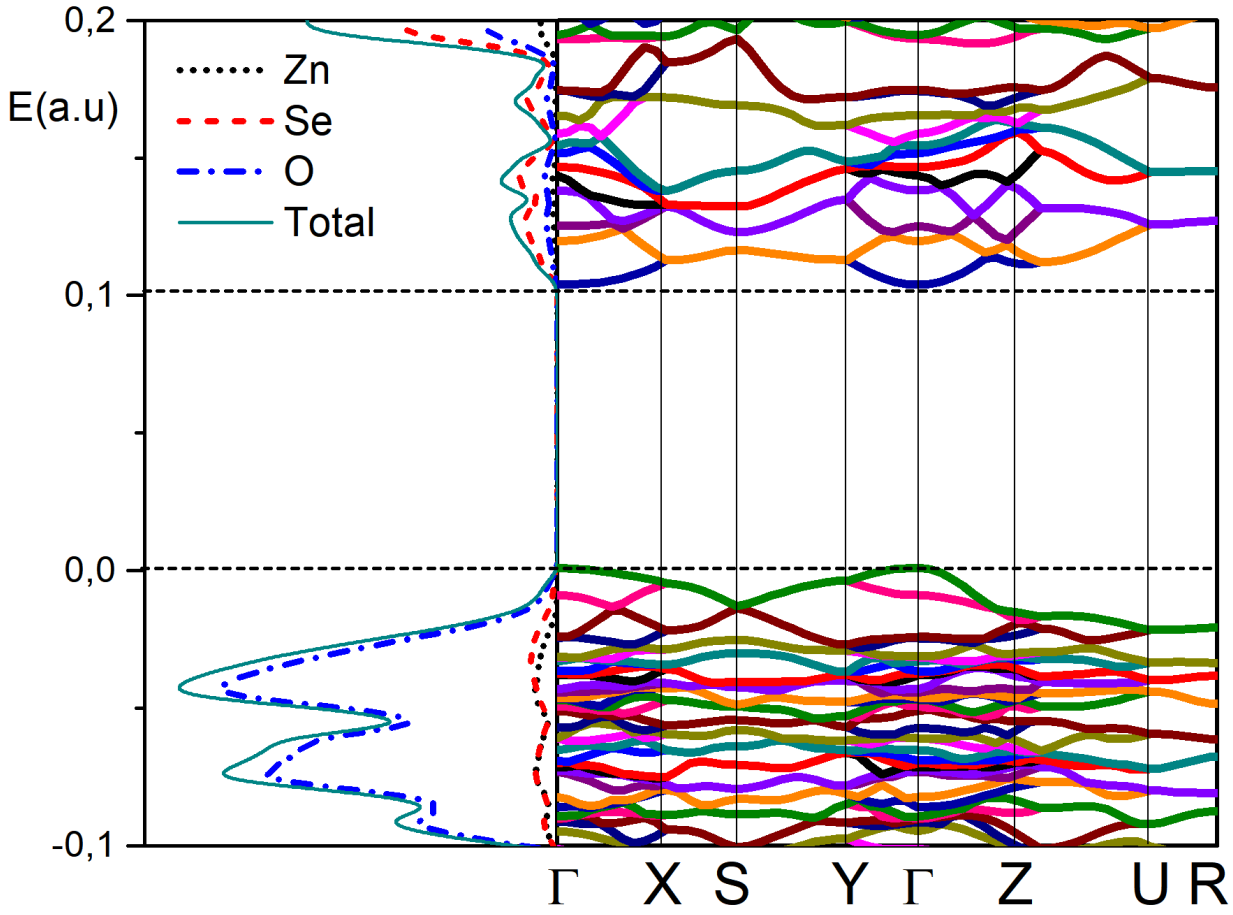

Fig. 3.

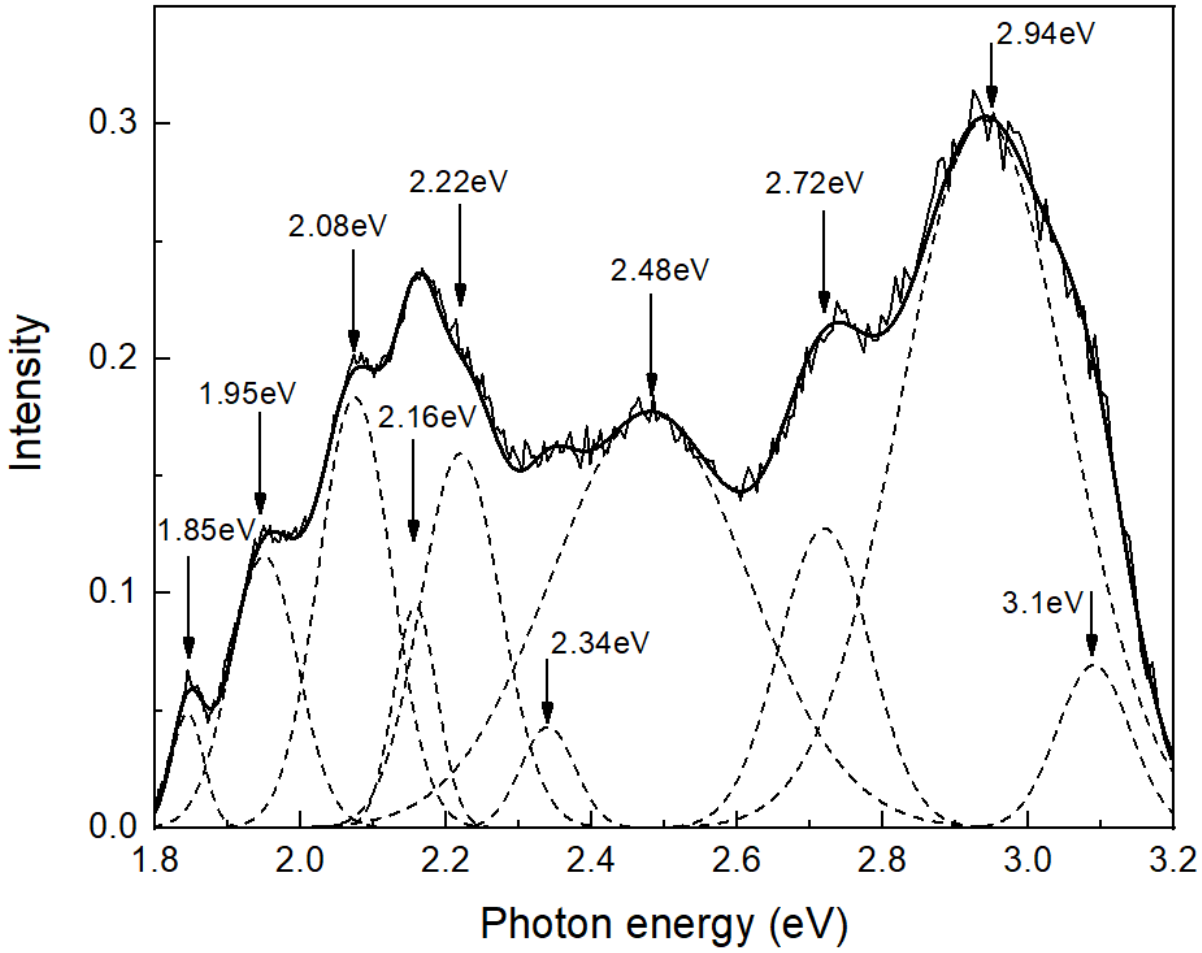

Fig. 4

Institute of Solid State Physics, University of Latvia as the Center of Excellence has received funding from the European Union's Horizon 2020 Framework Programme H2020-WIDESPREAD-01-2016-2017-TeamingPhase2 under grant agreement No. 739508, project CAMART²